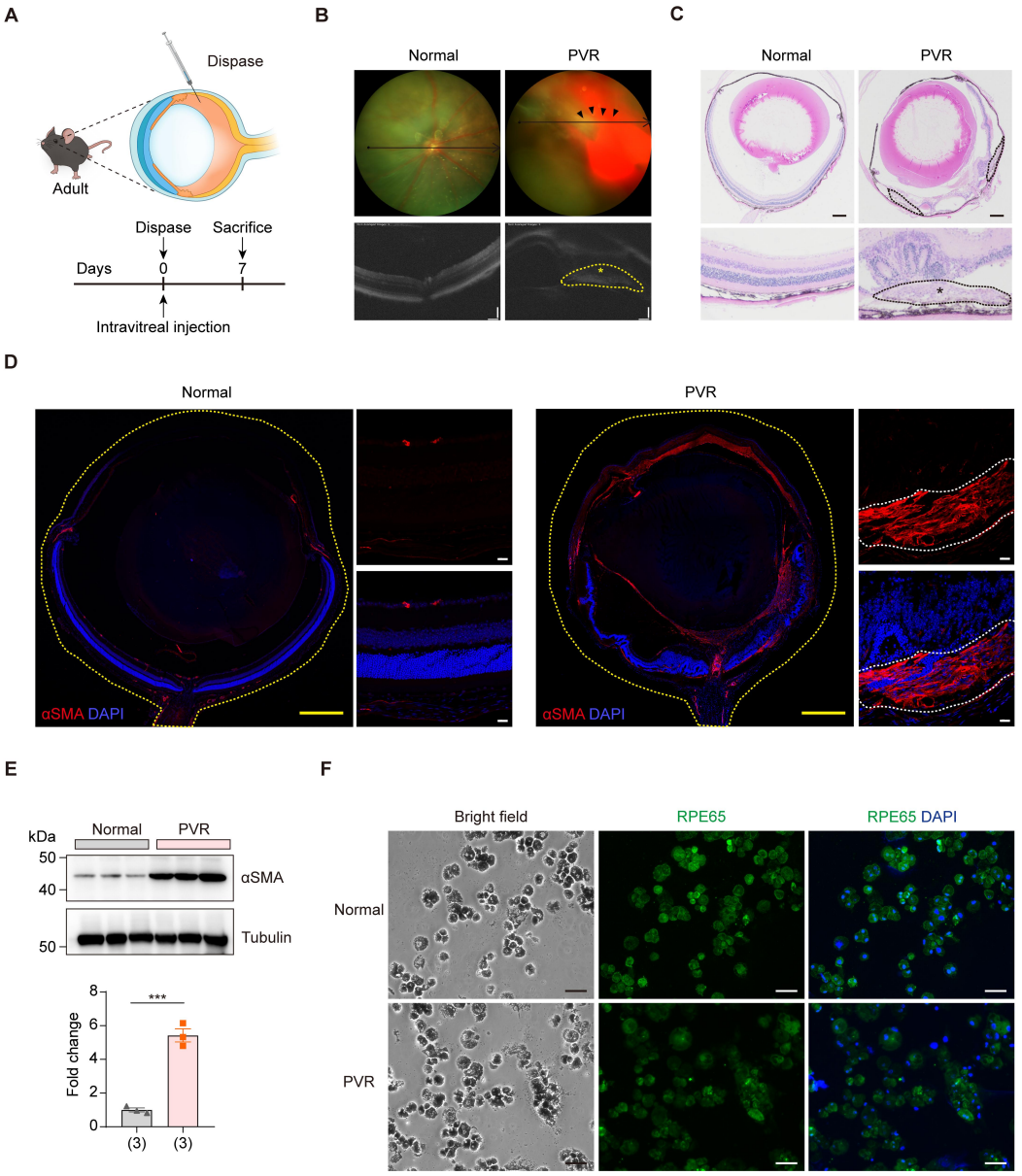

Supplementary Fig. 1 Establishment of a PVR mouse model. (A) Experimental strategy of PVR model. (B) Representative fundus imaging and OCT image of normal and PVR mice. The pathological changes were indicated with black arrows. The retinal fold or tractional area was circled with yellow dotted lines, and PVR membrane was marked with an asterisk (*). (C) Representative Hematoxylin and eosin (H&E) staining of eyeball sections.The black dotted lines indicated pathological changes, and PVR membrane was marked with an asterisk (*). Scale bars: 250 μm. (D) Representative immunofluorescent staining of αSMA in mouse eyeball sections. The yellow dotted lines indicated the whole eyeball. The white dotted lines indicated PVR membrane. Scale bars: yellow 100 μm, white 20 μm. (E) Western blot analysis (upper) and quantification (lower) of αSMA in eyecup tissues from normal and PVR mice. n=3 samples. Data are represented as means ± SEMs, and analyzed by two-tailed unpaired T test. ***$P < 0.001$. (F) Immunofluorescence staining of RPE65 in the isolated RPE cells. Scale bars: 50 μm.

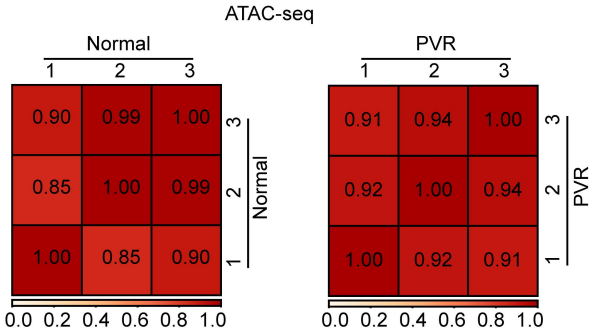

Supplementary Fig. 2 Evaluation of reproducibility across the ATAC-seq datasets in RPE cells. Heatmap displaying Spearman's correlation coefficient between biological replicates of ATAC-seq in normal and PVR RPE cells. Color intensity represents the strength of correlation.

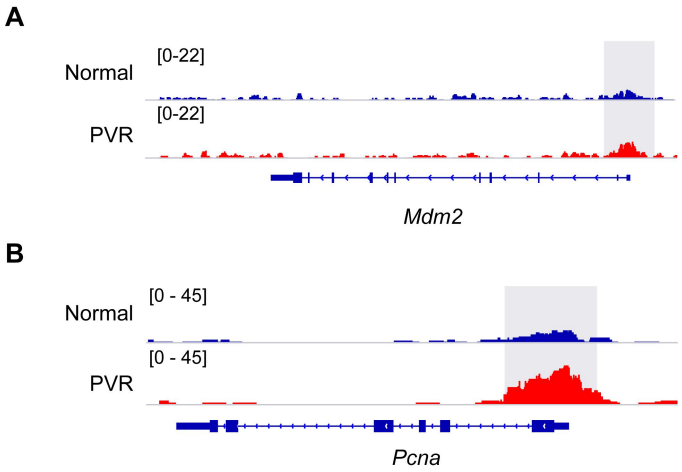

Supplementary Fig. 3 Integrative Genomics Viewer (IGV) track profiles of ATAC-seq. (A) IGV track profiles of ATAC-seq on *Mdm2*. (B) IGV track profiles of ATAC-seq on *Pcna*.

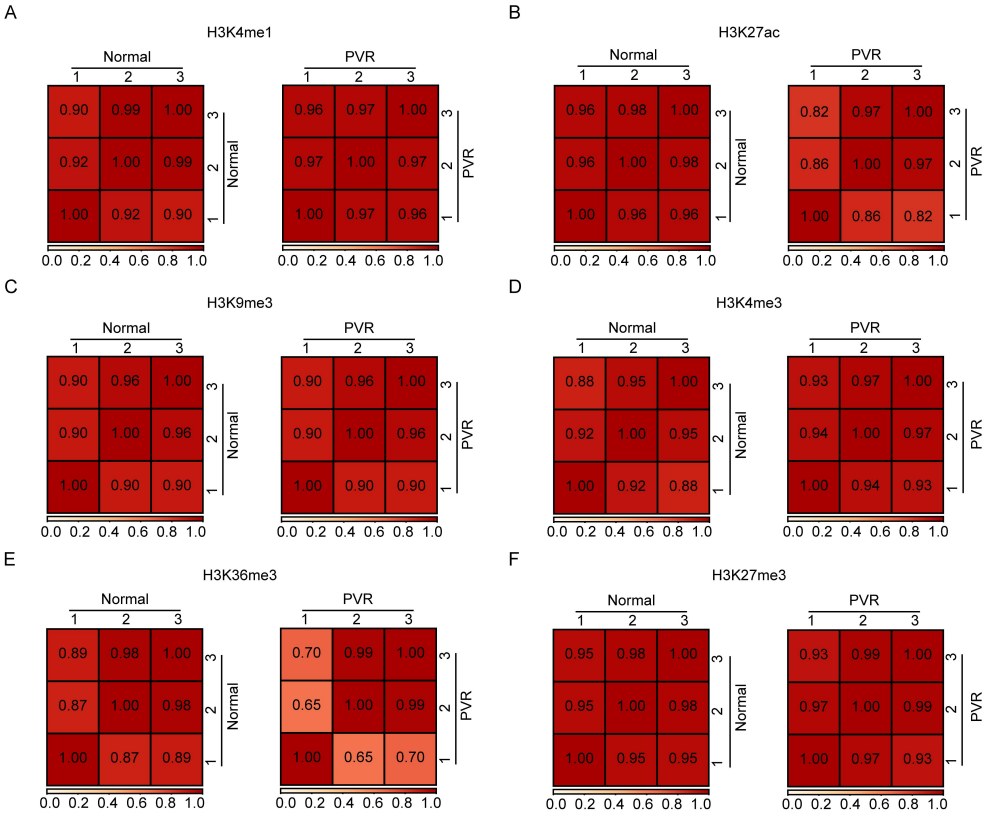

Supplementary Fig. 4 Evaluation of reproducibility across the ChIP-seq datasets in RPE cells. Heatmap displaying Spearman's correlation coefficient between biological replicates of (A) H3K4me1, (B) H3K27ac, (C) H3K9me3, (D) H3K4me3, (E) H3K36me3, and (F) H3K27me3 in normal and PVR RPE cells. Color intensity represents the strength of correlation.

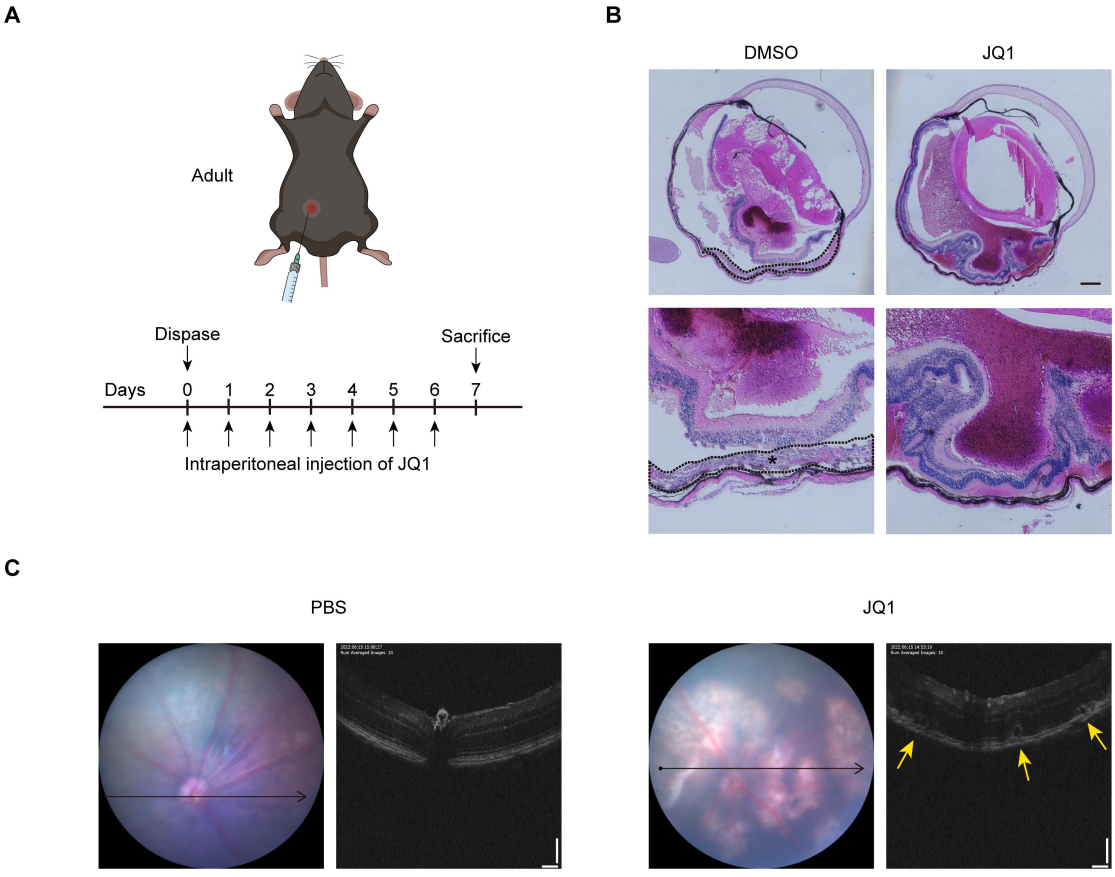

Supplementary Fig. 5 Effects and safety evaluation of JQ1 in DMSO. (A) Experimental strategy of PVR mice treated with DMSO and JQ1 in DMSO. (B) Representative H&E staining of eyeball sections from PVR mice treated with DMSO and JQ1 in DMSO. The black dotted lines indicated pathological changes, and PVR membrane was marked with an asterisk (*). Scale bar: 250 μm. This was repeated at least three times independently with similar results. (C) Representative fundus imaging and OCT image of mice treated with intraocular administration of PBS and JQ1 (218 μM) in DMSO. The lesion area was marked with yellow arrows. This was repeated at least three times independently with similar results.

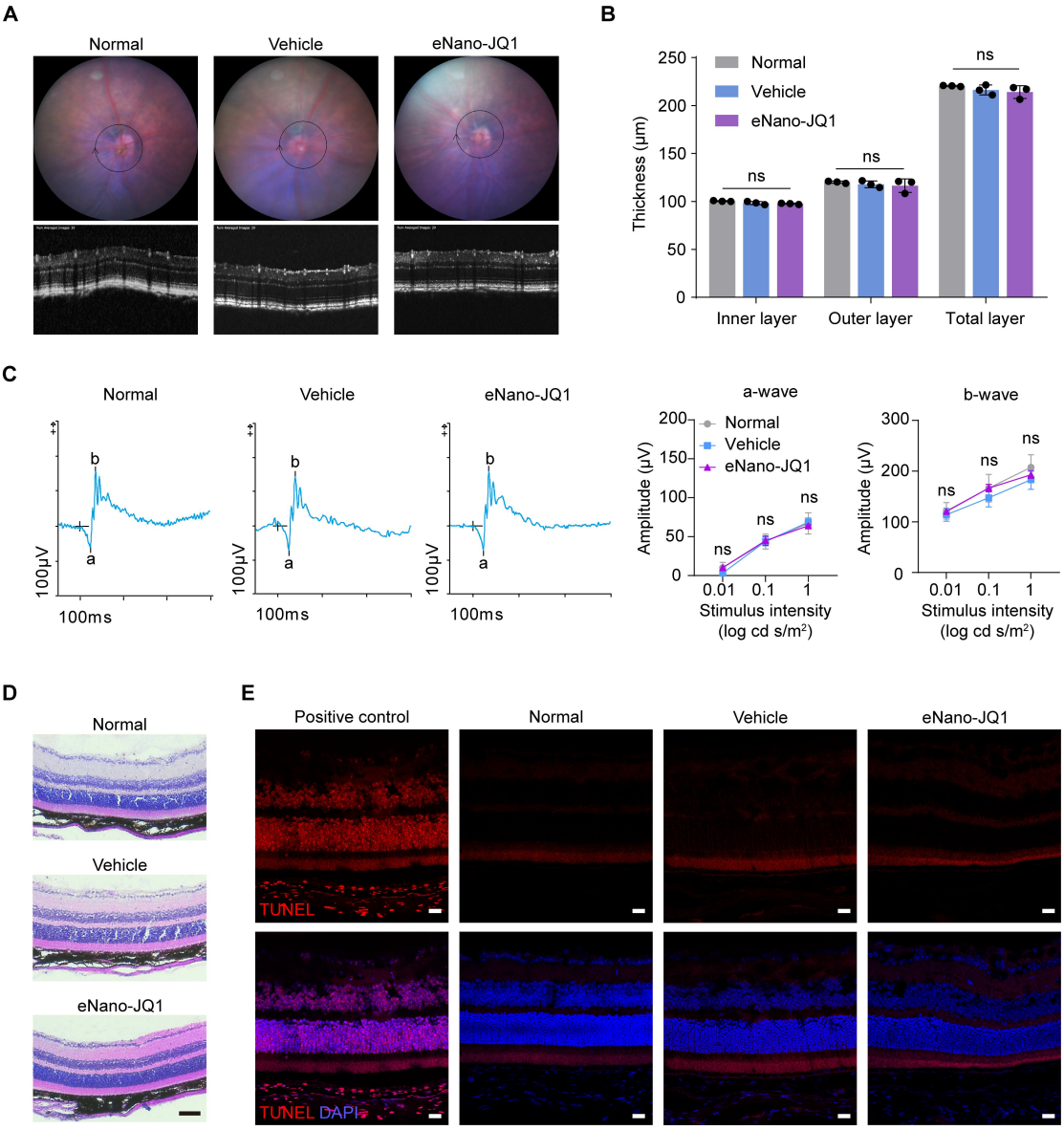

Supplementary Fig. 6 Safety evaluation of eNano-JQ1 via intraocular administration. (A) Representative fundus imaging and OCT image of normal mice and mice treated with vehicle or eNano-JQ1. (B) Thickness of inner, outer and total retinal layers. n=3 samples. Data are represented as means ± SEMs. *P* values were determined by one-way ANOVA multiple comparisons test, ns indicates $P \geq 0.05$. (C) Electroretinogram and quantification of normal mice and mice treated with vehicle or eNano-JQ1. n=3 samples. Data were represented as means ± SEMs. *P* values were determined by one-way ANOVA multiple comparisons test, ns indicates $P \geq 0.05$. (D) H&E staining of eyeball sections from normal mice and mice treated with vehicle or eNano-JQ1. Scale bar: 100 μm. (E) TUNEL assay of eyeball sections from normal mice and mice treated with vehicle or eNano-JQ1. Scale bars: 20 μm. (D) and (E) were repeated at least three times independently with similar results. Source data are provided as a Source Data file.

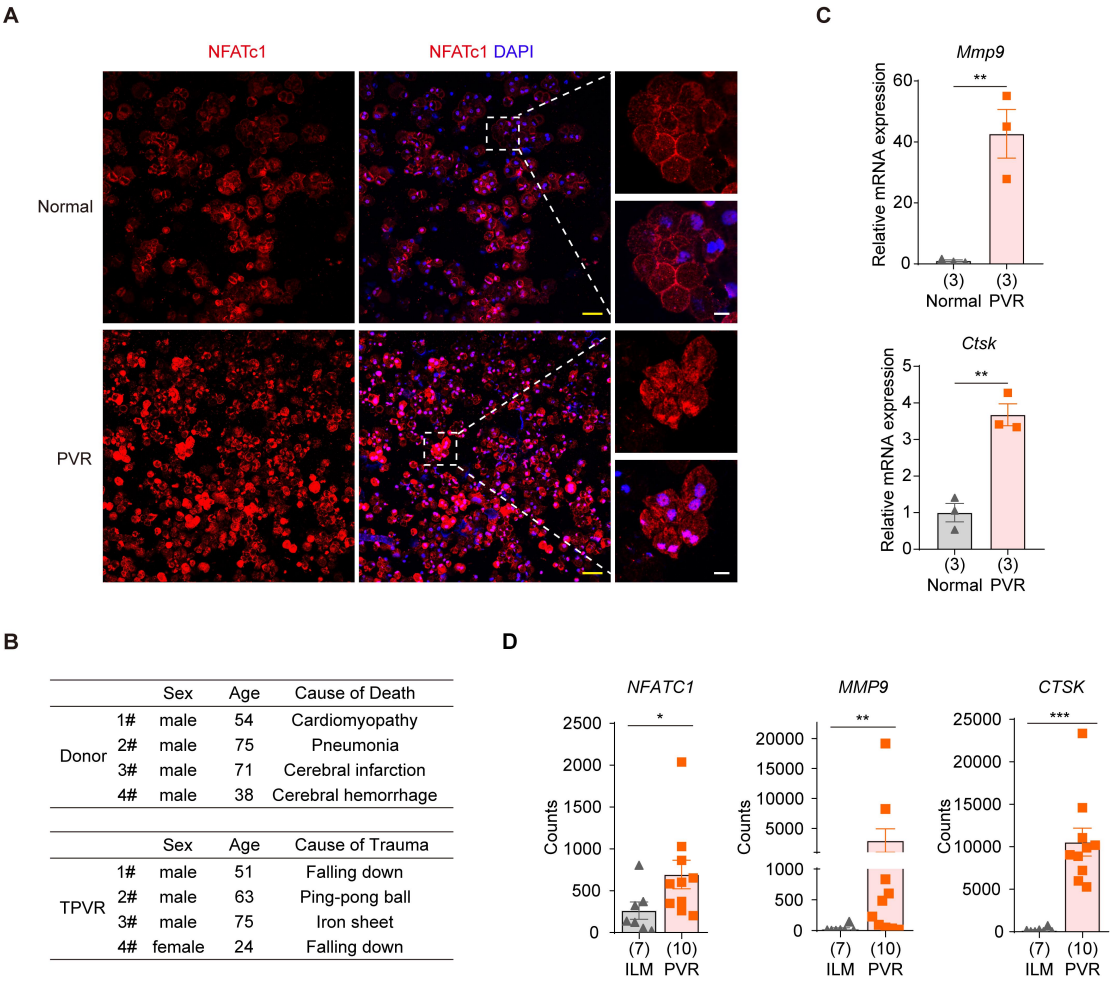

B

		Sex	Age	Cause of Death
Donor	1#	male	54	Cardiomyopathy
	2#	male	75	Pneumonia
	3#	male	71	Cerebral infarction
	4#	male	38	Cerebral hemorrhage

		Sex	Age	Cause of Trauma
TPVR	1#	male	51	Falling down
	2#	male	63	Ping-pong ball
	3#	male	75	Iron sheet
	4#	female	24	Falling down

Supplementary Fig. 7 Upregulation of NFATc1 and its target genes in PVR. (A) Representative immunofluorescence staining of NFATc1 in primary RPE cells from normal and PVR mice. Two selected areas (white dotted lines) are enlarged. Scale bars: yellow 100 μm, white 20 μm. This was repeated at least three times independently with similar results. (B) Clinical characteristics of the donors and traumatic PVR patients. (C) Quantitative RT-qPCR analysis of relative mRNA expression of *Mmp9* and *Ctsk* in primary RPE cells from normal and PVR mice. n=3 independent experiments. Data are represented as means ± SEMs, and analyzed by two-tailed unpaired T test. $^{**}P$ <0.01. (D) The mRNA expression of *NFATC1* and its indicated targets in PVR membrane and internal limiting membrane (ILM) from the publicly available RNA-seq data (GSE179603). n=7, 10 samples, respectively. Data are represented as means ± SEMs, and analyzed by by two-tailed Mann-Whitney test.. $^{*}P$ <0.05, $^{**}P$ <0.01, and $^{***}P$ <0.001. Source data are provided as a Source Data file.

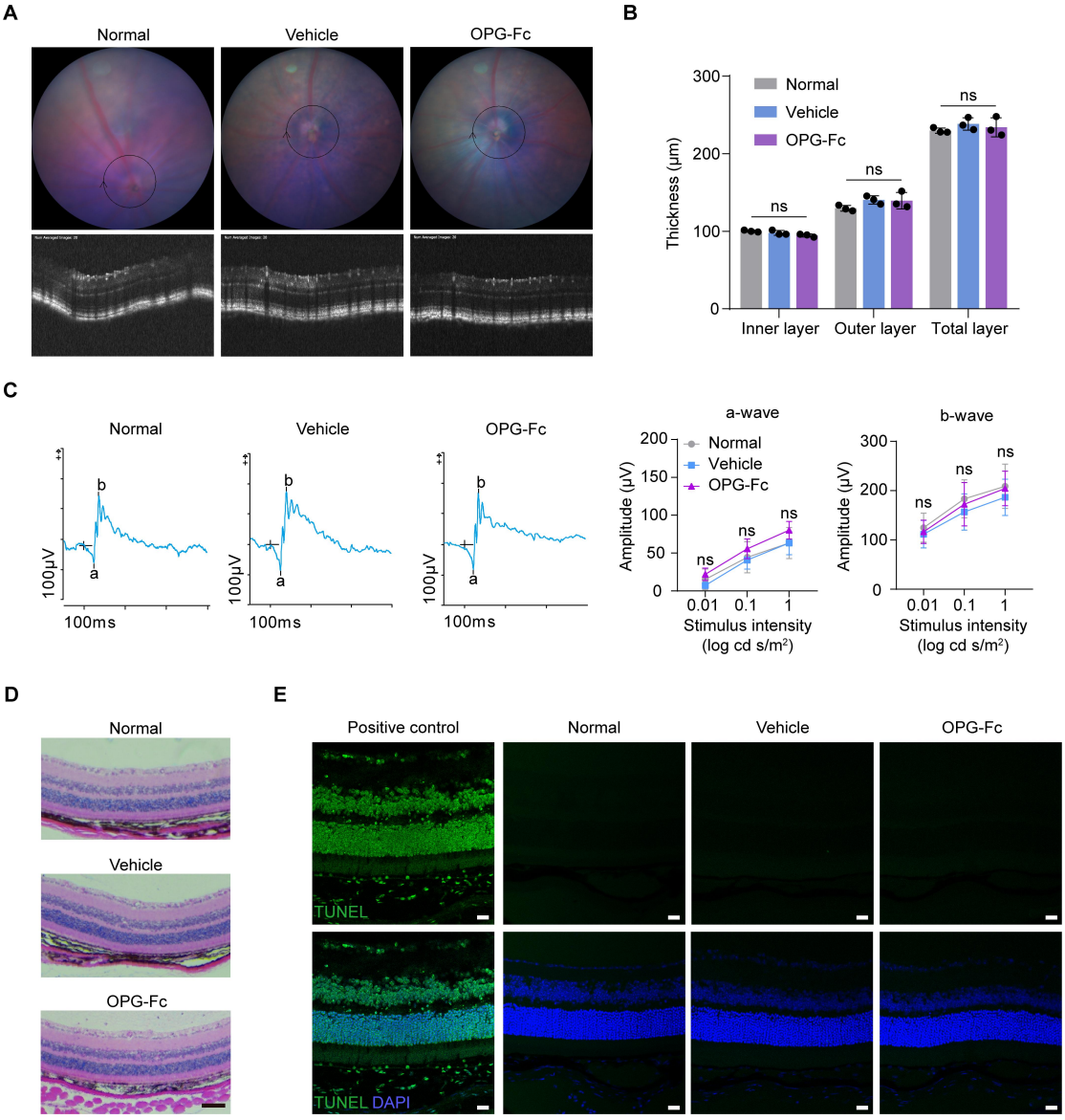

Supplementary Fig. 8 Safety evaluation of OPG-Fc via intraocular administration. (A) Representative fundus imaging and OCT image of normal mice and mice treated with vehicle or OPG-Fc. (B) Thickness of inner, outer and total retinal layers. n=3 samples. Data are represented as means ± SEMs. *P* values were determined by one-way ANOVA multiple comparisons test, ns indicates $P \geq 0.05$. (C) Electroretinogram and quantification of normal mice and mice treated with vehicle or OPG-Fc. n=3 samples. Data are represented as means ± SEMs. *P* values were determined by one-way ANOVA multiple comparisons test, ns indicates $P \geq 0.05$. (D) H&E staining of eyeball sections from normal mice and mice treated with vehicle or OPG-Fc. Scale bar: 100 μm. (E) TUNEL assay of eyeball sections from normal mice and mice treated with vehicle or OPG-Fc. Scale bars: 20 μm. (D) and (E) were repeated at least three times independently with similar results. Source data are provided as a Source Data file.

Supplemental Table 1. List of primers for RT- qPCR.

Gene name	Forward	Reverse
Nfatc1	ATGCCAAGTACCAGCTTTCCA	GGGACACATAACTGTAGTGTTCTTC
Mmp9	CTCTCCTGGCTTTCGGCTG	AGCGGTACAAGTATGCCTCTGC
Ctsk	GAAGAAGACTCACCAGAAGCAG	TCCAGGTTATGGGCAGAGATT
Rank	GGACAACGGAATCAGATGTGGTC	CCACAGAGATGAAGAGGAGCAG
Gapdh	TCAAGCTCATTTCCTGGTATGACA	TAGGGCCTCTCTTGCTCAGT

Full unedited gel for Supplementary Fig. 1E